# ELECTRICAL CHARACTERIZATION OF DEFECTS INTRODUCED IN n-GaN DURING HIGH ENERGY PROTON AND He-ION IRRADIATION

S. A. Goodman, F. D. Auret, F. K. Koschnick,[*] J.-M. Spaeth,[*] B. Beaumont[**] and P. Gibart[**]
Department of Physics, University of Pretoria, Pretoria 0002, South Africa
[*]Fachbereich Physik, Universität GH Paderborn, Paderborn, Germany
[**]CRHEA-CNRS, Valbonne, France.

**Cite this article as: MRS Internet J. Nitride Semicond. Res. 4S1, G6.12 (1999)**

## ABSTRACT

We report on the electrical properties of defects as determined by deep level transient spectroscopy (DLTS) introduced in epitaxially grown n-GaN by 2.0 MeV protons and 5.4 MeV He-ions. After He-ion bombardment three electron traps ER3 ($E_c$ - 0.196 eV), ER4 ($E_c$ - 0.78 eV), and ER5 ($E_c$ - 0.95 eV) were introduced uniformly in the region profiled by DLTS with introduction rates of $3270 \pm 200$, $1510 \pm 300$, and $3030 \pm 500$ $cm^{-1}$ respectively. Capture cross section measurements revealed that the electron capture kinetics of ER5 is similar to that of a line defect. A defect with similar electronic properties as ER3 is observed after 2.0 MeV proton irradiation. The emission rate of ER3 depends on the electric field strength in the space-charge region. This emission rate is modelled according to the Poole-Frenkel distortion of a square well with a radius of $20 \pm 2$ Å or alternatively, a Gaussian well with a characteristic width of $6.0 \pm 1$ Å. Hence, we conclude that ER1 is a point defect which appears to have an acceptor like character. Two additional electron traps, ER1 ($E_c$ - 0.13 eV) and ER2 ($E_c$ - 0.16eV) with introduction rates of $30 \pm 10$ and $600 \pm 100$ $cm^{-1}$ not thusfar observed after electron or He-ion bombardment were observed after proton irradiation.

## INTRODUCTION

Gallium nitride has recieved a great deal of attention due to its unique properties and is fast becoming an established material for wide band gap optoelectronic devices. It continues to show potential as a suitable material for high temperature and power applications [1]. It has unique applications in blue, green and ultraviolet light emitting diodes, detectors and blue lasers [2]. The device performance of several device types, including fast switches [3] and detectors [4], has been improved by subjecting the devices to controlled doses of particle irradiation. For this, and any other form of defect engineering, it is essential that the electronic properties of the defects involved should be known so that their influence on materials properties and device behaviour can be calculated. Further, the structure and composition of the defects should be known so that they can be reproducibly introduced. In the case of GaN, the investigation of particle induced defects is still in its infancy and only a few papers have appeared concerning the electrical characterisation of radiation induced defects.

Regarding studies of defects induced in GaN by high energy (MeV) particles, Linde *et al* have firstly reported that 2.5 MeV electrons introduced two broad photoluminescence bands in a 1 μm thick GaN/$Al_2O_3$ layer [5]. Thereafter, Look *et al* used Hall measurements to detect and identify the nitrogen vacancy at 0.07 eV below the conduction band in GaN,

https://doi.org/10.1557/S1092578300003124 Published online by Cambridge University Press

introduced during irradiation with 0.7 - 1.0 MeV electrons. [6] Subsequently, Fang *et al* observed, using deep level transient spectroscopy, that electron irradiation introduced a defect, which they labelled *E*, with a level at 0.18 eV below the conduction band. [7]

In this paper we report the introduction rates and electronic properties of defects introduced in n-GaN by 5.4 MeV He-ion and 2.0 MeV proton irradiation. The dependence of the emission rate on electric field strength of defect ER3 is presented and discussed and we also present the true capture cross section of a deep lying defect, ER5.

## EXPERIMENTAL PROCEDURE

For this study, 5 μm thick GaN epitaxial layers grown at $1080^0$C on a 250 Å GaN buffer layer on sapphire by metal-organic vapor phase epitaxy (MOVPE) were either exposed to 5.4 MeV He-ions from a $^{241}$Am radio-nuclide source or 2.0 MeV protons from a Van de Graaff accelerator. The nominally undoped GaN epitaxial layer had a free carrier concentration of approximately 2 - 3 x $10^{16}$ $cm^{-3}$. After boiling the samples in aqua-regia for ten minutes the samples were degreased [8]. Prior to ohmic contact fabrication the oxide layer was removed form the sample surface using a $HCl : H_2O$ (1 : 1) solution for 10 seconds [9]. The composite ohmic contact layer [10] was Ti/Al/Ni/Au (150 Å/2200 Å/400 Å/500 Å). The contact fabrication was followed by a five minute anneal at 500 $^o$C in an inert gas atmosphere. Gold Schottky barrier diodes (SBDs), 0.5 mm in diameter and 3000 Å thick were resistively deposited, these diodes had reverse leakage currents of the order of $10^{-10}$ A at 1 V and ideality factors between 1.05 and 1.10. The samples were exposed to 5.4 MeV He-ions by placing them on an $^{241}$Am foil. The activity of the radionuclide being 192 μCi.$cm^{-2}$ and the dose rate was 7.1 x $10^6$ $cm^{-2}.s^{-1}$. Sampes exposed to 2.0 MeV protons in the Van de Graaff accelerator recieved a dose of (3 ± 1) x $10^{11}$ $cm^{-2}$ at a dose rate of approximately 1 x $10^{10}$ $cm^{-2}s^{-1}$. A two-phase lock-in-amplifier-based (LIA) deep level transient spectroscopy (DLTS) system was used for the defect characterization in the as-grown material and the particle bombarded material. In order to simplify the determination of the emission kinetics of ER3 at different electrical field strengths in the space-charge region, isothermal DLTS was used.

## RESULTS AND DISCUSSION

Fig. 1 depicts the DLTS spectra of control (curve (a)), 5.4 MeV He-ion irradiated (curves (b & c)) and 2.0 MeV proton irradiated (curves (d & e)) epitaxial n-GaN. Consider the spectra for the as-grown material (curve (a)). In this defect labelling nomenclature, "E" implies electron trap and "O" that the material was grown by MOVPE. From the literature it appears that EO2 and EO5 are the same as the E1 and E2, respectively, observed by Hacke *et al* in n-GaN grown by hydride vapor-phase epitaxy [11]. These two defects also have similar sigantures as $E_2$ and $E_1$, respectively, detected by Götz *et al* in MOCVD grown GaN [12]. After exposing the GaN to 5.4 MeV He-ions, three prominent additional defects, ER3, ER4 and ER5, were observed (curves (b) and (c) in Fig. 1), defects, ER4 and ER5, were detected after recording DLTS spectra using a filling pulse frequency of 100 mHz, i.e. an emission rate of about 0.23 $s^{-1}$. The DLTS signatures of ER4 and ER5 were determined (Table I and Fig. 2) by using pulse frequencies of between 4.6 and 220 mHz. Note that under "typical" DLTS recording conditions (emission rates of 50 - 200 $s^{-1}$) the DLTS peaks of ER4 and ER5 would

https://doi.org/10.1557/S1092578300003124 Published online by Cambridge University Press

occur at (430 – 450 K) and (470 – 500 K) respectively, which is probably why they were not previously detected.

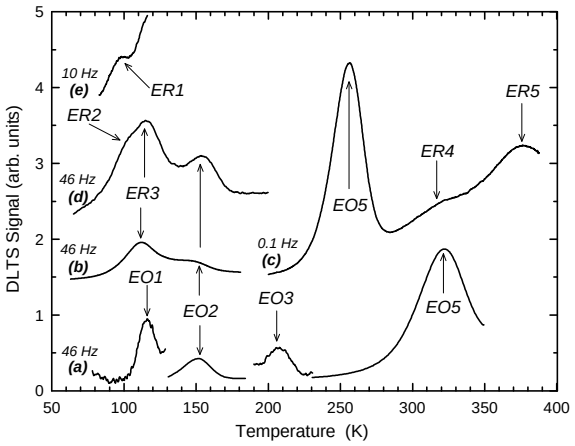


**Figure 1:** Curve (a): DLTS spectrum of as-grown MOVPE n-GaN. Curves (b) and (c): spectra recorded after 5.4 MeV He-ion irradiation. Curves (d) and (e): spectra recorded after 2.0 MeV proton irradiation. Curves (a) – (c) were recorded using a reverse bias ($V_r$) of 2.0 V and filling pulse amplitudes ($V_p$) of 2.2 V. For curves (d) and (e), $V_r$ = 2.0 V and $V_p$ = 0.5 V.

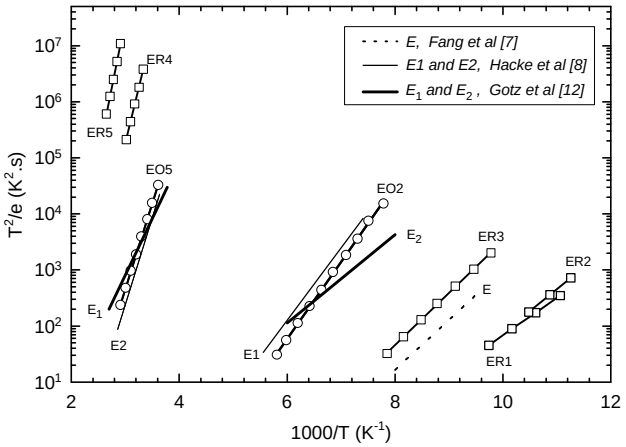


**Figure 2:** DLTS Arrhenius plots of defects in as grown n-GaN (open circles) and high ebergy He-ion and proton irradiation (open squares). Other lines are for defects detected in GaN by other authors.

**TABLE I.** Electronic properties of defects introduced in epitaxial n-GaN by 5.4 MeV He-ion and 2.0 MeV proton irradiation.

| Defect label | $E_T$ (eV) | $s_{na}$ ($cm^2$) | $T_{peak}$[(a)] (K) | $h$ ($cm^{-1}$) | Similar defects |
|---|---|---|---|---|---|
| EO1 | 0.21 | $4\times10^{-14}$ | 114 | grown in | |
| EO2 | 0.27 | $8\times10^{-15}$ | 156 | grown in | E1[11] |
| EO3 | 0.45 | $7\times10^{-13}$ | 208 | grown in | |
| EO5 | 0.61 | $1\times10^{-14}$ | 322 | grown in | E2 [11] |
| ***2.0 MeV PROTON*** | | | | | |
| ER1 | 0.13 | $2\times10^{-16}$ | 98 | 30±10 | |
| ER2 | 0.16 | $4\times10^{-15}$ | 103 | 400±150 | |
| ER3 | 0.20 | $4\times10^{-15}$ | 121 | 600±100 | E [7], $V_{Ga}N_i^{2-}$ [14] |
| ***5.4 MeV He-ION*** | | | | | |
| ER3 | 0.20 | $4\times10^{-15}$ | 121 | 3270±200 | E [7], $V_{Ga}N_i^{2-}$ [14] |
| ER4 | 0.78 | $1\times10^{-15}$ | 323[(b)] | 1510±300 | —— |
| ER5 | 0.95 | $3\times10^{-14}$ | 377[(b)] | 3030±500 | $N_i$ [13]$_i$ $V_{Ga}N_i^-$ [14] |

*[(a)] Peak temperature at a LIA frequency of 46 Hz, i.e. an emission rate of 108 $s^{-1}$. [(b)] Peak temperature at 0.1 Hz*

The levels of ER4 ($E_C$ - 0.78 eV) and ER5 ($E_C$ - 0.95 eV) are the deepest radiation induced levels below the conduction band yet detected by DLTS. The only radiation induced defect related transitions with roughly the same energy as the ER4 and ER5 are those reported by Linde *et al* after a photoluminescence (PL) study of electron irradiated GaN [5]. These authors found that electron irradiation introduces two PL bands centred around 0.85 and 0.93 eV, respectively, and using optically detected magnetic resonance, they tentatively identified the latter as a $Ga_I^{2+}$-complex. Due to the fundamental differences in the origin of DLTS and PL spectra, no direct comparison between their PL and our DLTS spectra is possible.

https://doi.org/10.1557/S1092578300003124 Published online by Cambridge University Press

However, since Ga interstitials are formed during irradiation, they, or complexes including them, are likely to yield deep levels which can be detected by DLTS. Alternative possibilities for structure of ER5 is the N-interstitial, which was predicted to result in levels near the center of the band gap [13], and the $V_{Ga}N_i^-$ and $V_{Ga}N_i^{2-}$ states with levels calculated to be in the upper half of the bandgap [14].

Curves (d) and (e) in Fig. 1, recorded using different filling pulse conditions, show that proton bombardment introduces the defects ER1 – ER3. Defect, ER1 could only be clearly detected when using pulse widths, $t_p$, of less than 2 μs. Using a filling pulse width of $t_p$ = 400 ns, we have determined the activation energy of ER1 as 0.13±0.01 eV below the conduction band (Fig. 2). For pulse widths larger than 1 μs, the ER3 peak appears and seems to reach a maximum for a pulse width of about 1 ms at 121 K, indicating that ER3 has a small electron capture cross section.

As the ER3 amplitude grows with increasing pulse width, it obscures the detection of the much smaller ER1 peak. When increasing the pulse width to above 1 ms, the ER3 peak showed a broadening. The extraordinary large pulse widths required to detect ER2 indicate that its real electron capture cross section is even smaller that of ER3 (unlike their almost identical apparent capture cross-sections).

The signature of ER3 was determined using $t_p$ = 50 μs. This pulse width yields a strong ER3 signal but it is too narrow for ER2 to capture a significant amount of carriers and thus to contribute to the DLTS signal at the temperatures where we studied ER3. The energy level thus determined, $E_C$ - 0.20±0.01 eV, is similar to that of a defect, labelled *E*, with a level at $E_C$ - 0.18 eV, observed by Fang *et al* [7] after electron irradiation of MOVPE (metal-organic vapor phase epitaxy) grown GaN. These authors pointed out that, should this defect have a temperature activated capture cross section, its actual position in the bandgap may be close to that of $V_N$ ($E_C$ - 0.07) [6], but no firm identification has yet been made. To extract the electronic properties of ER2, spectra which were recorded at different frequencies, using pulses just sufficient to saturate ER3, were subtracted from spectra recorded with a wide enough pulse to clearly show the ER2 signal. This procedure yielded an activation energy of 0.16±0.03 eV.

In Fig. 3 the experimentally measured emission rate of ER3 as a function of the square root of the electric field in the space charge region is shown. In order to establish the potential associated with this defect the experimental data was modelled making use of various simple defect potential models. It would appear that the square well and the gaussian well with their particular physical dimensions, both provide an adequate description of defect ER3. In an attempt to understand how both potentials describe the experimental results, a comparison of the distortion of these potentials at a reasonably high (2.5 x $10^5$ V/cm) electric field strength was investigated. Figure 4 schematically represents the distortion of a square and a gaussian well. It is clear from this figure that using either a gaussian or a square well with the specified physical attributes can adequately describe the enhanced emission kinetics of ER3.

Capture cross section ($s_n$) measurements of ER5 were performed using pulse widths, $t_p$, of between 50 ns and 50 ms. As shown in Fig. 5, the DLTS signal of ER5 increased monotonically with $t_p$ for the whole pulse width range investigated. Because the total concentration of radiation induced defects in the sample used for this measurement was much lower than the free carrier concentration, this incomplete filling of ER5 is not due to a competition for electrons between ER5 and the shallow donors. The presence of a straight line region in the plot of ΔC/C vs log(*t*) in Fig. 5 is similar to what has been observed for

https://doi.org/10.1557/S1092578300003124 Published online by Cambridge University Press

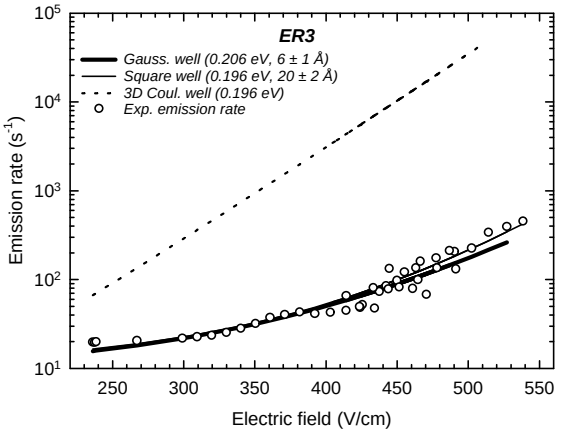


**Figure 3:** The experimental and modelled emission kinetics of defect ER3 as a function of electric field strength in the space charge region.

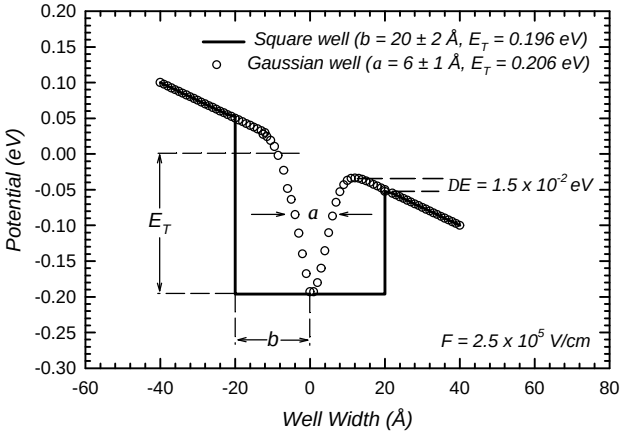


**Figure 4:** The reduction in potential for a gaussian and a square well, when the electric field strength in the space charge region is $2.5 \times 10^5$ V/cm.

carrier capture by traps which are *not randomly* distributed, but which are arranged along lines [15]. In such a case the capture rate is limited by a Coulomb barrier which increases with increasing charge capture onto the extended defects. The data presented here strongly suggests that ER5 is a line defect, or an extended defect, where charge build-up governs the capture rate.

Regarding the formation mechanism for such a defect, it should be noted that 5.4 He-ions can transfer sufficient energy to the GaN lattice to cause defect spikes or extended regions of disorder.

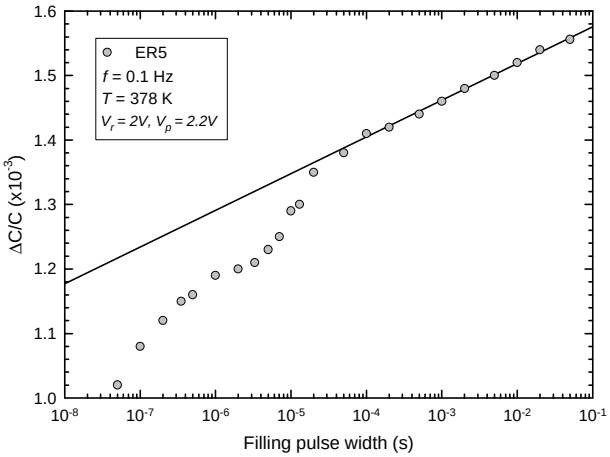


**Figure 5:** DLTS signal (S(t) = ΔC/C) as function of log(t) for ER5. The error in S(t) is about the same as the height of the symbol.

## CONCLUSIONS

In conclusion, we have determined the electronic properties of 4 electron defects (EO1 – EO3, EO5) present in as-grown MOVPE n-GaN. This material was then subjected to high energy He-ion or proton irradiation, wherupon additional electron defects were introduced. After the 5.4 MeV He-ion irradiation 3 additional defects (ER3 – ER5) were measured. The emission charateristics of defect ER3 does not exhibit the typical dependence on $F^{½}$ that is classicaly used to determine the electronic type of the defect. The temperature dependance of the capture cross-section of defect, ER5 suggests that it may be a line or an extended defect. After 2.0 MeV proton irradiation 3 defects (ER1 – ER3) were observed. Thusfar the major proton irradiation induced defect ER2 has not been observed in similar material exposed to high energy He-ions. Defect ER3 is similar to that observed after 5.4 MeV He-ion irradiation.

## ACKNOWLEDGMENTS

https://doi.org/10.1557/S1092578300003124 Published online by Cambridge University Press

We gratefully acknowledge financial assistance from the South African Foundation for Research Development. We also thank G. Myburg for ohmic contact metallisation and W.E. Meyer for assistance with the isothermal DLTS measurements.

## REFERENCES

[1] K. Doverspike, A. E. Wickenden, S. C. Binarii, D. K. Gaskill and J. A. Freitas, Mat. Res. Soc. Symp. Proc. Vol. 395, p897 (1996).
[2] S. Nakamura and G. Fasol, in "The blue laser diode", (Springer Verlag, 1997).
[3] M. Lambsdorff, J. Kohl, J. Rosenzweig, A. Axmann and J. Schneider, Appl. Phys. Lett. 58, 1881 (1991).
[4] V. M. Rao, W-P Hong, C. Caneau, G-K. Chang, N. Papanicolaou, and H. B. Dietrich, J. Appl. Phys. 70, 3943 (1991).
[5] M. Linde, S.J. Uftring, G.D. Watkins, V. Harle and F. Scholz, Phys. Rev. B 55, R10177 (1997).
[6] D.C. Look, D.C. Reynolds, J.W. Hemsky, J.R. Sizelove, R.L. Jones and R.J. Molnar, Phys. Rev. Lett. 79, 2273 (1997).
[7] Z-Q. Fang, D. C. Look, W. Kim, Z. Fan, A. Botchkarev and H. Morkoc, Appl. Phys. Lett. 72, 2277 (1998).
[8] P. Hacke, T. Detchprohm, K. Hiramatsu, and N. Sawaki, Appl. Phys. Lett. 63, 2676 (1993).
[9] J.K. Sheu, Y.K. Su, G.C. Chi, W.C. Chen, C.Y. Chen, C.N. Huang, J.M. Hong, Y.C. Yu, C.W. Wang, and E.K. Lin, J. Appl. Phys. 83, 3172 (1998).
[10] S. Ruminov, Z. Liliental-Weber, J. Washburn, K.J. Duxstad, E.E. Haller, Z.-F. Fan, S.N. Mohammed, W. Kim, A.E. Botchkarev, and H. Morkoc, Appl. Phys. Lett. 69, 1556 (1996).
[11] P. Hacke, T. Detchprohm, K. Hiramatsu and N. Sawaki, Appl. Phys. Lett. 63, 2676, (1993).
[12] W. Götz, N. M. Johnson, H. Amano and I. Akasaki, Appl. Phys. Lett. 65, 463 (1994).
[13] J. Neugebauer and C.G. Van de Walle, Phys. Rev. B 50, 8067 (1994).
[14] T. Mattila, A.P. Seitsonen and R.M. Nieminen, Phys. Rev. B 54, 1474 (1996).
[15] T. Wosinski, J. Appl. Phys. 65, 1566 (1988).

https://doi.org/10.1557/S1092578300003124 Published online by Cambridge University Press